

## Effects of stoichiometry on electrical, optical, and structural properties of indium nitride

J. C. Ho,<sup>a)</sup> P. Specht, Q. Yang, X. Xu, D. Hao, and E. R. Weber

*Materials Sciences Division, Lawrence Berkeley National Laboratory, Berkeley, California 94720 and Department of Materials Science and Engineering, University of California, Berkeley, California 94720*

(Received 19 May 2005; accepted 3 October 2005; published online 10 November 2005)

A series of indium nitride (InN) epilayers with different excess indium (In) concentration are grown by plasma-assisted molecular-beam epitaxy on (0001) sapphire substrates. The increasing excess In concentration of the epilayers correlates with an increasing free-electron concentration and a decreasing electron mobility. Photoluminescence (PL) illustrates a 0.77–0.84 eV transition for all samples with a redshift in the peak energy with increasing In concentration (for the highest free-electron concentration of  $4 \times 10^{21} \text{ cm}^{-3}$ ). This suggests that the  $\sim 0.8$  eV PL transition is not consistent with the band-edge transition in InN. Moreover, an additional PL transition at 0.75 eV along with the In clusters observed in transmission electron microscopy analysis are found only in the 29% excess In sample. This implies a relationship between the new PL transition and the presence of In clusters. Finally, secondary-ion mass spectrometry is used to verify that the contamination, especially hydrogen (H) and oxygen (O) impurities, has no influence on the redshift of the  $\sim 0.8$  eV PL peaks and the existence of the additional 0.75 eV peak in the sample containing In clusters. © 2005 American Institute of Physics. [DOI: 10.1063/1.2130514]

### INTRODUCTION

Indium nitride (InN) is a challenging but promising semiconductor among the group III-nitride compounds. Due to the lack of suitable substrates, both the lattice constant and the coefficient of thermal-expansion mismatch induce high defect concentrations during the heteroepitaxial growth of InN. The high equilibrium vapor pressure of nitrogen for InN limits the deposition temperature. The low growth temperature of  $\sim 500$ – $600$  °C results in high defect concentrations and, therefore, a poor crystal quality for highly mismatched heterosystems. Recently, with various improved growth techniques, InN epilayers with low free-electron concentration ( $\sim 10^{17} \text{ cm}^{-3}$ ) and high electron mobility ( $\sim 2100 \text{ cm}^2/\text{Vs}$ ) have been produced,<sup>1</sup> which may lead to future high-speed electronic applications. Since then, a series of research efforts have been focused on the fundamental band gap of InN. The variations in the band-gap measurements were mainly attributed to the Burstein-Moss energy shift,<sup>2</sup> the presence of oxide precipitates,<sup>3,4</sup> the formation of indium (In) clusters<sup>5</sup> and other stoichiometry-related defects.<sup>6</sup>

In this paper, the effect of excess In incorporation on the electrical, optical, and structural properties of InN is investigated. By keeping a constant nitrogen flux, the effect of a stoichiometry variation can be investigated while maintaining a constant background contamination level. The contamination, especially of oxygen, is believed to be correlated to residual nitrogen gas impurity and is monitored by secondary-ion mass spectrometry (SIMS) analysis.

### EXPERIMENT

InN epilayers are grown by molecular-beam epitaxy (MBE) in a Riber 1000 system. The substrates used are (0001) sapphire wafers with backside sputter-coated titanium metal for efficient heat absorption during the growth. A standard indium (In) effusion cell and a dc nitrogen plasma source are used.<sup>7</sup> Plasma operating conditions are 740 V, 100 mA, and 30 SCCM (standard cubic centimeter per minute)  $\text{N}_2$  flow. The substrate temperature is determined by pyrometry, taking the substrate emissivity as 0.9. Common growth rates are about  $0.3 \mu\text{m}/\text{h}$ . Prior to the epitaxial growth, the substrates are thermally cleaned at 800 °C for 20 min and then nitridated at 650 °C for 30 min. A very thin In metal layer ( $\sim 5$  nm) is deposited at 275 °C with the effusion cell temperature of 800 °C and then annealed in a nitrogen plasma environment for 7 min and 30 s with the substrate temperature being ramped to 535 °C simultaneously. Finally, a series of InN epilayers is grown with In cell temperatures ranging from 815 to 830 °C, resulting the epilayers' thickness in about 0.7–0.9  $\mu\text{m}$ .

### RESULTS AND DISCUSSION

Figure 1(a) shows the high-resolution x-ray-diffraction (HRXRD) normal-coupled scans for five samples grown with increasing In cell temperatures. The (0002) InN and (0006) sapphire reflections are at  $31.4^\circ$  and  $41.7^\circ$ , respectively, for all samples. For increasing In cell temperatures, the (101) reflection of metallic In at  $33.0^\circ$  becomes stronger. The increasing indium-to-nitrogen flux ratio during epitaxy results in a segregation of pure metallic indium within the crystal (indium clusters) or on the surface layer. The percent-

<sup>a)</sup> Author to whom correspondence should be addressed; present address: 330 HMMB, University of California, Berkeley, CA 94720; electronic mail: jcho@berkeley.edu

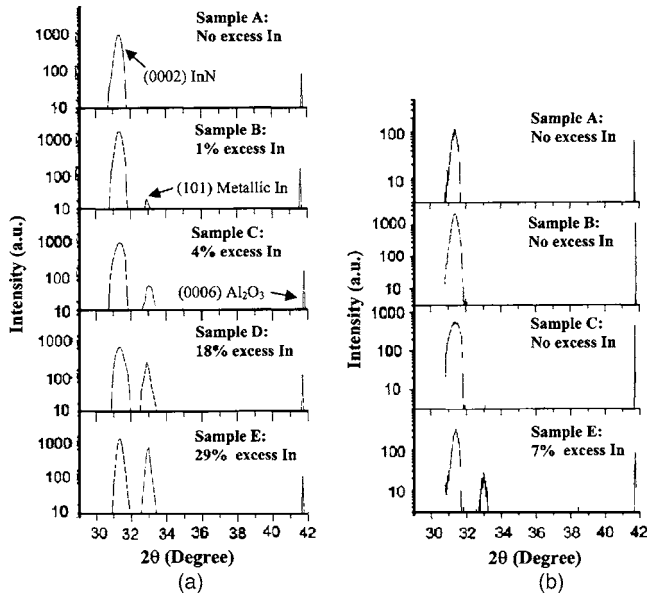


FIG. 1. (a) HRXRD-coupled-normal scans for samples grown with increasing In cell temperatures before etching (Left). (b) After etching (Right).

age of excess In deposition, also shown in Fig. 1(a), is determined by the fraction of area of the metallic (101) In peak over the (0002) InN peak.

The influence of excess In incorporation on electrical properties is investigated. As presented in Fig. 2, the free-electron concentration increases from  $1 \times 10^{20}$  to  $4 \times 10^{21} \text{ cm}^{-3}$  while the electron mobility decreases from 210 to  $40 \text{ cm}^2/\text{Vs}$  as the concentration of excess In is increased. Sample E (29% excess In) shows 39% error in the measurements of free-electron concentration and electron mobility while other samples have error less than 10% in the Hall measurements. The error is due to the significant surface conduction which will be discussed below, but this error does not affect the trend as shown in Fig. 2.

The relationship between the excess In incorporation and the electrical properties suggests that the presence of excess In provides free carriers to the crystal and forms defects, likely In clusters as reported before,<sup>5</sup> which act as electron-

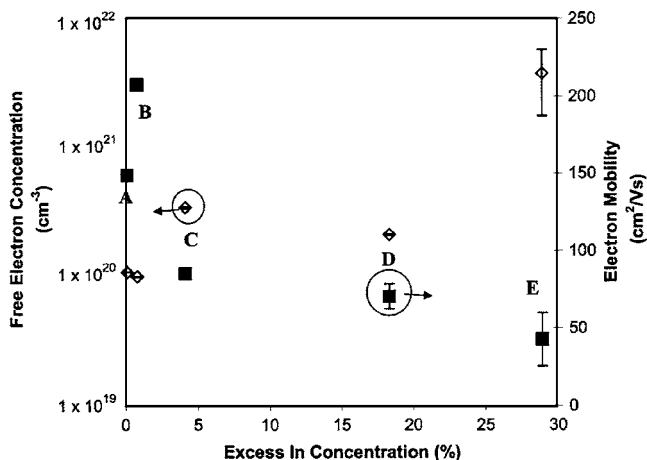


FIG. 2. The free-electron concentration and the electron mobility vs the excess In concentration. (filled square: mobility; open diamond: electron concentration).

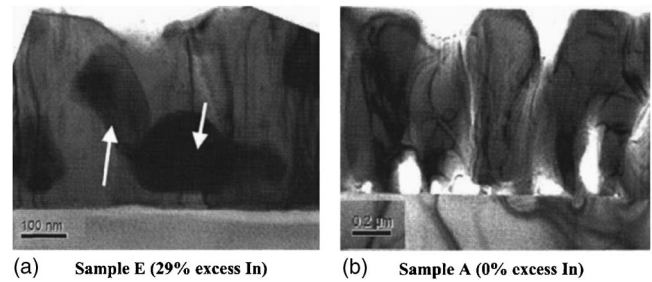


FIG. 3. (a) TEM image of Sample E (left). (b) TEM image of sample A (right).

scattering centers. If the excess In would accumulate entirely on the surface layer, the increase of the free-electron concentration suggests that the surface conduction is dominant. However, the electron mobility decreases with increasing excess In, which can only be described by a bulk conduction mechanism. These multiple conduction mechanisms of bulk, surface, and interface in InN epilayers were also reported by Swartz *et al.*<sup>8</sup> The observations above suggest that the excess In segregates at least partly as a form of In clusters in the bulk crystal but may also partly segregate on the surface of the epilayers.

In order to locate the excess In in the samples, all samples are etched in  $\text{HCl}:\text{H}_2\text{O}$  (1:3) solution to remove any indium on the top surface as reported by Lu *et al.*<sup>9</sup> while the thickness of the epilayers are not affected. Figure 1 shows the comparison of the HRXRD normal-coupled scans before and after etching all samples. As depicted in Fig. 1(b), the (101) metallic In reflections have been disappeared in all the scans except for sample E (29% excess In). Sample E has 7% residual excess In left within the bulk while 22% of excess In are removed from the surface. Unfortunately, sample D is destroyed during the sample preparation; the reproduction of the sample is in progress.

After the surface etching, the Hall data of samples A and B is unchanged while the free-electron concentration of sample C decreases from  $3.5 \times 10^{20}$  to  $1.5 \times 10^{20} \text{ cm}^{-3}$  and the electron mobility increases from 85 to  $145 \text{ cm}^2/\text{Vs}$ . However, the available area of sample E is too small for the Hall measurement; no further conclusion between the bulk and surface conductivity can be obtained from the Hall data here.

Sample A and sample E are investigated by transmission electron microscopy (TEM) in an effort to locate incorporated excess indium. As demonstrated in Fig. 3(a), there are clusters visible within the crystal as pointed out by the white arrows. Electron energy loss spectroscopy (EELS) is performed to identify the chemical composition of the clusters. They appear to be pure metallic indium since only the indium  $M_{4,5}$ -absorption edge at 460 eV is observed and the nitrogen  $K$ -absorption edge expected at 401 eV is not detected. An EELS spectrum taken from the In cluster is shown in Fig. 4. It shall be noted that we are aware of the knock-on-type damage with ejection of nitrogen atoms by electron beams as reported in scanning transmission electron microscopy of InN.<sup>10</sup> However, Fig. 3(b) does not show any presence of clusters in sample A (0% excess In) using the same

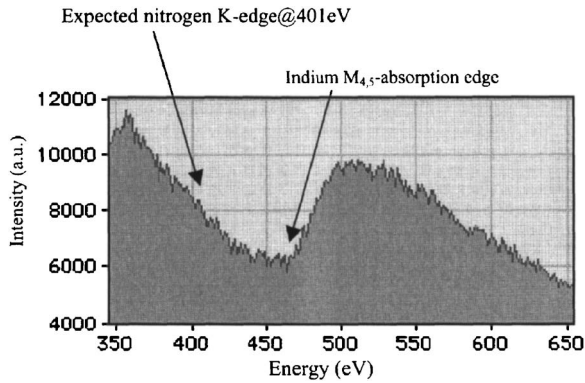


FIG. 4. EELS spectrum of the In cluster in sample E.

sample preparation procedures and imaging condition, suggesting that the In clusters detected in sample E are not caused by artifacts from the sample preparation or electron-beam damage. Summarizing the above observations, it is assumed that the formation of In clusters in the InN crystal exists as another mechanism to incorporate excess metallic In besides the well-known—and for lower excess indium concentrations likely dominant—indium deposition on the epilayer's surface. The HRXRD diffraction peak at  $2\theta \sim 33^\circ$  also proved to associate with the surface In layer or the In clusters in the bulk in our samples, which is not necessarily related to the polycrystalline InN films reported in the literature.<sup>11</sup>

Figures 5(a) and 5(b) present the low-temperature (15 K) photoluminescence (PL) of all samples before and after etching. A 514.5 nm Ar<sup>+</sup> laser with a power density of

200 W/cm<sup>2</sup> was used as the excitation source. A liquid-nitrogen-cooled germanium photodetector was used for the photon energy range of 0.7–1.2 eV. All samples show a PL transition at around 0.8 eV before and after the etching. As the surface In concentrations are removed from the samples, the PL intensities of the excess In samples increase relative to the 0% sample. It is an expected effect since the indium surface layer is believed to scatter the incoming radiation for the PL measurement. The origin of the PL transitions commonly observed in InN between 0.6 and 0.8 eV is still controversially discussed. Various research groups<sup>12–14</sup> which positions the fundamental band gap of InN around 0.7 eV, suggest the 0.7–0.8 eV PL peak to be the band-edge transition. Others<sup>3,5,15</sup> attribute this low-energy transition to an extrinsic recombination process analogous to the process that gives a blue band in aluminum nitride and a yellow band in gallium nitride, exciton emissions in the In-rich interfaces and In clustering in the InN epilayers.

As shown in Fig. 5(c), the peak energies for samples C to E vary slightly before and after etching, suggesting that the indium surface layer may induce the slight energy shifts. This unexpected effect is still investigated. The peak energies clearly exhibit a redshift from sample B (1% excess In) to sample E (29% excess In) before and after etching. This redshift of the PL peak cannot be explained by the Burstein-Moss shift,<sup>2</sup> as our samples show increasing free-electron concentration with increased excess In. Moreover, according to the Burstein-Moss shift theory for InN, the investigated samples here should have a PL band-edge transition at 1.2 eV or above—for free-electron concentrations between

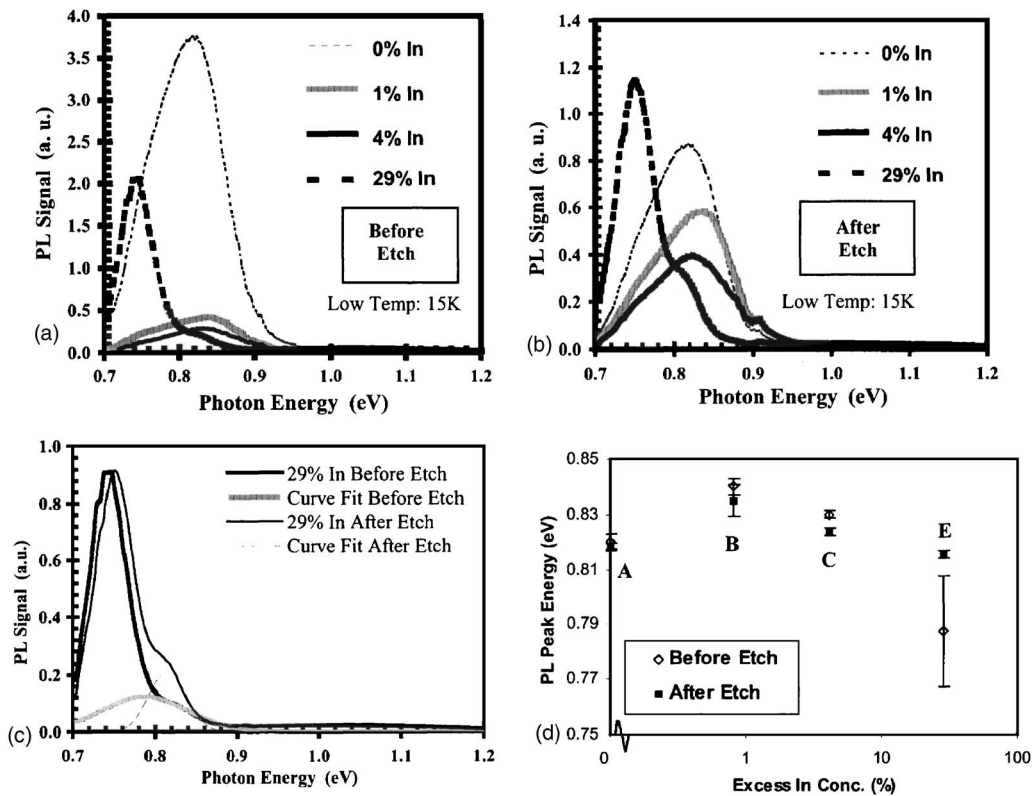


FIG. 5. (a) PL of samples before etching (top left). (b) PL of samples after etching (top right). (c) PL peak energies of samples (center; open diamond: before etching; filled square: after etching). (d) PL spectra for sample E (20% excess In sample) with curves fitted for the  $\sim 0.8$  eV peak (bottom).

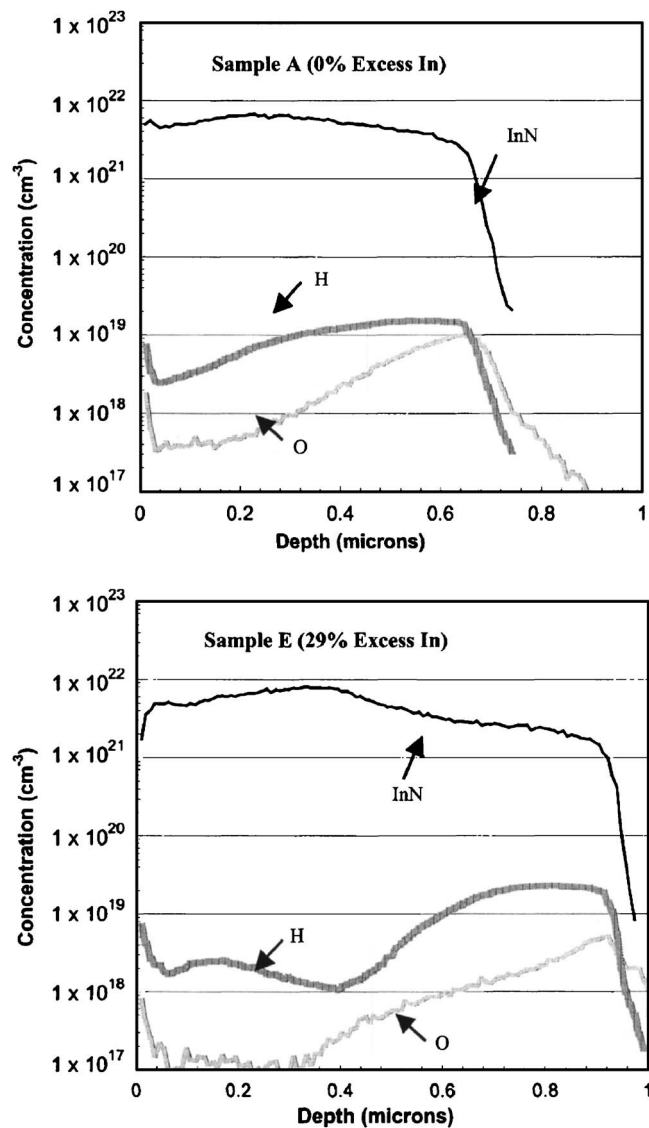


FIG. 6. SIMS profiles of samples A and E. (top: sample A; bottom: sample E)

$1 \times 10^{20}$  and  $4 \times 10^{21} \text{ cm}^{-3}$ —instead of around 0.8 eV as observed here. As a result, the PL at around 0.8 eV observed here is not consistent with a band-to-band transition.

In addition to the redshift, as shown in Fig. 5(d), there is an additional PL transition at 0.75 eV for sample E which is not observed in the other samples. This peak remains after etching indicating that this additional transition at lower energy is indeed related to the bulk instead of the indium surface layer. The observation of In clusters in this particular sample may be connected to the PL at 0.75 eV. This finding agrees well with the bright IR (0.7–0.8 eV) PL emission associated with the In aggregates in InN epilayers reported by Shubina *et al.*<sup>5</sup> This is not the first example relating PL to metal clusters. The effect of green luminescent ruthenium clusters with PL centered at 2.4 eV has been studied on the optical application of chemically derivatized porous silicon.<sup>16</sup>

Figure 6 shows the SIMS profiles of sample A (0% excess In) and sample E (28.9% excess In). The oxygen (O) and hydrogen (H) concentrations are calibrated.<sup>17</sup> The InN

profile provides the location of the epilayer and therefore also gives an estimate of the film thickness. It was found that the two epilayers were deposited with different growth rates,  $0.28 \mu\text{m/h}$  for sample A and  $0.36 \mu\text{m/h}$  for sample E. This unexpected side effect is still under investigation. The average hydrogen and oxygen concentrations are very similar between those two samples. They are about  $1 \times 10^{19}$  and  $1 \times 10^{18} \text{ cm}^{-3}$ , respectively. Since the MBE growth is an ultra-high vacuum process, samples are not expected to consist of all kinds of impurities; indeed, other impurity concentrations such as Mg, B, Cl, C, S, and Si are also measured by SIMS and those impurities do not exist in any significant level. As a result, the free-electron concentration of the two samples is almost one order of magnitude higher than the total concentration of H and O, indicating that the major source of unintentional donors is not impurity related. Surface or interface charge accumulation<sup>9</sup> and native defects such as nitrogen vacancies<sup>18</sup> are likely candidates for the unexplained high level of background *n*-type conductivity. In addition, the SIMS results verify that the redshift of the  $\sim 0.8 \text{ eV}$  PL peaks and the additional PL transition at 0.75 eV in sample E are not associated with a change in hydrogen and/or oxygen contamination level.

## CONCLUSION

It was shown that the incorporation of excess In increases the free-electron concentration and decreases the electron mobility in InN. Mixed conduction effects are expected due to the multiple conducting layers of bulk, surface, and interface. With photoluminescence, a transition at around 0.8 eV was found for all samples. A redshift in the PL peak energy was observed with increasing excess In and free-electron concentration. This suggests that the observed PL transition here at around 0.8 eV is not correlated to a band-to-band transition. In addition, when the incorporation of excess In is greater than 22% on the surface, the formation of indium clusters is confirmed by TEM. Those In clusters coincide with an additional PL transition at a lower energy of 0.75 eV suggesting that this emission is In aggregates associated.

## ACKNOWLEDGMENT

This work was supported by the Director, Office of Science, Office of Basic Energy Sciences, Materials Sciences and Engineering Division, of the U.S. Department of Energy under Contract No. DE-AC02-05CH11231, and the Air Force Office of Scientific Research under Contract No. FA9550-04-1-0408.

<sup>1</sup>H. Lu, W. J. Schaff, L. F. Eastman, J. Wu, W. Walukiewicz, D. C. Look, and R. J. Molnar, *Mater. Res. Soc. Symp. Proc.* **743**, L4.10.1 (2003).

<sup>2</sup>J. Wu, W. Walukiewicz, W. Shan, K. M. Yu, J. W. Ager, E. E. Haller, L. Hai, and W. J. Schaff, *Phys. Rev. B* **66**, 201403 (2002).

<sup>3</sup>D. Alexandrov, K. Scott, A. Butcher, and M. Wintrebert-Fouquet, *J. Vac. Sci. Technol. A* **22**, 954 (2004).

<sup>4</sup>M. Yoshimoto, H. Yamamoto, H. Wei, H. Harima, J. Saraie, A. Chayahara, and Y. Horino, *Appl. Phys. Lett.* **83**, 3480 (2003).

<sup>5</sup>T. V. Shubina *et al.*, *Phys. Rev. Lett.* **92**, 117407 (2004).

<sup>6</sup>K. S. A. Butcher *et al.*, *J. Appl. Phys.* **95**, 6124 (2004).

<sup>7</sup>P. Specht, R. Armitage, J. Ho, E. Gunawan, Q. Yang, X. Xu, C.

- Kisielowski, and E. R. Weber, *J. Cryst. Growth* **269**, 118 (2004).
- <sup>8</sup>C. H. Swartz, R. P. Tompkins, N. C. Giles, T. H. Myers, L. Hai, W. J. Schaff, and L. F. Eastman, *J. Cryst. Growth* **269**, 29 (2004).
- <sup>9</sup>H. Lu, W. J. Schaff, L. F. Eastman, and C. E. Stutz, *Appl. Phys. Lett.* **82**, 1736 (2003).
- <sup>10</sup>K. A. Mkhoyan and J. Silcox, *Appl. Phys. Lett.* **82**, 859 (2003).
- <sup>11</sup>K. M. Yu *et al.*, *Appl. Phys. Lett.* **86**, 071910 (2005).
- <sup>12</sup>V. Y. Davydov *et al.*, *Phys. Status Solidi B* **229**, R1 (2002).
- <sup>13</sup>J. Wu *et al.*, *Appl. Phys. Lett.* **80**, 3967 (2002).
- <sup>14</sup>Y. Nanishi, Y. Saito, and T. Yamaguchi, *Jpn. J. Appl. Phys., Part 1* **42**, 2549 (2003).
- <sup>15</sup>O. Briot, B. Maleyre, S. Clur-Ruffenach, B. Gil, C. Pinquier, F. Demangeot, and J. Frandon, *Phys. Status Solidi C* **6**, 1425 (2004).
- <sup>16</sup>R. Boukherroub, D. Zargarian, C. Reber, D. J. Lockwood, A. J. Carty, and D. D. M. Wayner, *Appl. Surf. Sci.* **217**, 125 (2003).
- <sup>17</sup>J. Wu *et al.*, *Appl. Phys. Lett.* **84**, 2805 (2004).
- <sup>18</sup>C. Stampfl, C. G. Van de Walle, D. Vogel, P. Kruger, and J. Pollmann, *Phys. Rev. B* **61**, R7846 (2000).